Scientific Research Publishing

Pharmacology & Pharmacy, 2023, 14, 123-143
https://www.scirp.org/journal/pp
ISSN Online: 2157-9431
ISSN Print: 2157-9423

Development and Evaluation of Stable Paracetamol Loaded Solid Dispersion with Enhanced Analgesic and Hepatoprotective Property

Ashim Kumar[1], Milon Kumar Ghosh[2], Mst. Boby Aktar Bithy[1], Md. Rafiqul Islam Khan[1], Md. Monimul Huq[3], Mir Imam Ibne Wahed[1], Ranjan Kumar Barman[1*]

[1]Laboratory of Pharmaceutics, Department of Pharmacy, Faculty of Science, University of Rajshahi, Rajshahi, Bangladesh
[2]Department of Pharmacy, Faculty of Biological Sciences, Islamic University, Kushtia, Bangladesh
[3]Department of Statistics, Faculty of Science, University of Rajshahi, Rajshahi, Bangladesh
Email: *drbarman76@gmail.com

How to cite this paper: Kumar, A., Ghosh, M.K., Bithy, M.B.A., Khan, M.R.I., Huq, M.M., Wahed, M.I.I. and Barman, R.K. (2023) Development and Evaluation of Stable Paracetamol Loaded Solid Dispersion with Enhanced Analgesic and Hepatoprotective Property. *Pharmacology & Pharmacy*, **14**, 123-143.
https://doi.org/10.4236/pp.2023.144010

Received: March 26, 2023
Accepted: April 25, 2023
Published: April 28, 2023

Abstract

Paracetamol (PCM) is enlisted in the WHO model list as an essential medicine for pain and palliative care, but at overdose, it causes hepatic damage. This study was designed to assess the analgesic efficacy and hepatoprotective property of a solid dispersion (SD) loaded with PCM. A number of PCM loaded formulations (PSDs) were fabricated using silica alone or in combination with polyethylene glycol and/or Na-citrate followed by *in-vitro* dissolution profiling. Selected PSDs with improved dissolution profile were subjected to solid-state characterization (DSC, PXRD, FTIR, and SEM), stability study along with investigation of *in-vivo* analgesic efficacy and effect on hepatocytes. Among these, PSD10 showed a rapid and significantly higher *in-vitro* drug release than pure PCM. This improvement was distinct to other PSDs also. Solid-state characterization of PSD10 authenticated the conversion of crystalline PCM to amorphous form upon formulation. Subsequent oral administration of PSD10 in Swiss albino mice showed 1.44-fold greater analgesic efficacy than pure PCM at dose 30 mg/kg. Besides, at acute toxic dose, liver histology of PSD10 mice was comparable with NC mice indicating hepatic protection upon formulation, whereas the PCM mice showed extensive hepatic necrosis which was also endorsed by significantly higher values of SGPT, SGOT, and ALP than PSD10 mice. Finally, an accelerated stability study of PSD10 performed according to the guideline of ICH noticed no remarkable deviation in its dissolution performance as well as crystalline nature. Thus, this newly developed PSD10 may be a safe and promising alternative for pain management and palliative care.

Keywords

Paracetamol, Solid Dispersion, Dissolution, Analgesic Activity, Hepatocyte, Particle Surface Property, Stability

1. Introduction

Paracetamol (PCM), chemically known as N-(4-hydroxyphenyl) acetamide (**Figure 1**) is a widely used oral analgesic and antipyretic drug [1]. It is mostly considered to be a weak inhibitor of prostaglandin synthesis that has been used customarily in mild to moderate pain management for decades [2] [3] [4]. Conventional PCM is sparingly soluble (14 mg/ml at 20˚C) in water with 70% - 90% bioavailability after oral administration [5] [6] [7]. Around 90% of the administered PCM is directed to phase II metabolic pathways in the liver and undergoes glutathione, sulfate, and glucuronide conjugation [7]. But the depletion of these metabolic enzymes, particularly glutathione leads to marked hepatotoxicity through the formation of the noxious NAPQI metabolite, which is a common clinical feature of PCM overdose [8] [9] [10].

In limited doses, PCM is very safe but the margin of safety is relatively narrow, leading to dose-dependent liver injury in mammals [11]. It was found that the hepatotoxicity can be reduced by modified drug particles achieved with drug delivery systems (DDSs), *i.e.*, nanotechnology related to the altered metabolic pathways in the liver [12] [13]. These findings facilitated further development and clinical translation of DDSs. Rapid dissolution and absorption of PCM are crucial to achieve quick onset of drug action by applying various tailored formulations or technologies. Some recently used approaches to improve dissolution profileare incorporation of PCM into porous lactose, solid dispersion (SD) formulation, engineered PCM crystal and nanotechnology [4] [14]-[19]. Of these, SD is used extensively to enhance *in-vitro* drug release by reducing particle size, amorphous conversion, altered surface property, and others which offered SD as a promising DDS for the study to investigate the hepatic impact of PCM in the formulation [20] [21] [22]. Moreover, improved *in-vitro* drug release profile, as well as *in-vivo* bioavailability of drug entities, is achieved with SD by manipulation of the carrier, by changing particle size distribution, by enhancing the wettability and porosity of drug molecules, and by polymorphic change [23] [24]. This technology has also become victorious to develop formulations with a high loading capacity of drugs tending to re-crystallize [25].

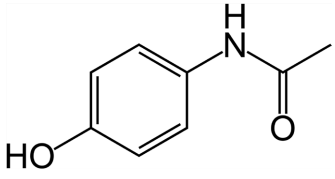

Figure 1. Structure of paracetamol (Source: Wikipedia).

Therefore, this study aimed to appraise the therapeutic potential of PCM and hepatic toxicity by offering a new and stable paracetamol loaded solid dispersion (PSD) approach.

2. Materials and Methods

2.1. Materials

PCM was a kind gift from Square Pharmaceuticals Ltd., Pabna, Bangladesh. Carplex-67 (silica) was purchased from Evonik Pvt. Ltd. (Hanua, Germany). Polyethylene glycol-4000 (PEG-4000), methanol, ethanol, and Na-citrate were procured from Qualikems Fine Chem Pvt. Ltd. (India). Dialysis tubing (Fisherbrand™ Regenerated Cellulose Dialysis Tubing, MWCO 12,000 - 14,000 d and, diameter 1.125 inches) was purchased from Fisher Scientific, USA. All other chemicals, and reagents used were of analytical grade.

2.2. Preparation of PSDs

SDs of PCM with silica as a carrier or in combination with PEG and/or Na-citrate at different weight ratios was prepared using solvent evaporation technique. In brief, accurately weighed (200 mg) PCM was dissolved in sufficient quantity of ethanol, into which silica at different ratios was added (Table 1). Before incorporation, PEG was separately dissolved in ethanol and Na-citrate was dissolved in a small quantity of water. Then the drug-carrier dispersion was dispersed under continuous stirring by a hot plate magnetic stirrer at 200 rpm to allow sufficient loading of the drug into carriers. The temperature was maintained at 50˚C - 60˚C to evaporate the solvent from the dispersion system. When the evaporation of the solvent was near to be completed, the magnetic stirrer was stopped. PSDs were obtained as a dried powder at room temperature. The PSDs were passed through a mesh screen and stored for further experiments.

Table 1. Solid dispersion formulations at different ratio of drug and carriers.

Groups	Solid dispersions	Drug & Carrier	Formulation ratio
1	PSD1	PCM:silica	1:1
	PSD2	PCM:silica	1:2
	PSD3	PCM:silica	1:3
2	PSD4	PCM:silica:PEG	2:2:1
	PSD5	PCM:silica:PEG	1:1:1
	PSD6	PCM:silica:PEG	1:1:2
3	PSD7	PCM:silica:Na-citrate	2:2:1
	PSD8	PCM:silica:Na-citrate	1:1:1
	PSD9	PCM:silica:Na-citrate	1:1:2
Optimized	PSD10	PCM:silica:PEG:Na-citrate	1:1:1:1

2.3. Determination of Encapsulation Efficiency (EE)

To determine the EE, PSD was weighed theoretically equivalent to 30 mg PCM and was transferred to a 100 ml volumetric flask. To this, 20 - 30 ml of methanol was added, shaken gently and the volume was made up to 100 ml with methanol followed by filtration through Whatmann filter paper no.1. The filtrate was diluted to obtain the theoretical concentration of 30 µg/ml and then absorbance was measured with a UV-spectrophotometer (UVmini-1240, Shimadzu) at λ_{max} 243.5 nm. The drug content was determined using a calibration curve constructed with 5 standard concentrations (10, 20, 30, 50, and 100 µg/ml) of PCM. The percentage EE was calculated and repeated in triplicate to obtain the mean value [26].

2.4. *In-Vitro* Dissolution Profiling

The *in-vitro* dissolution profiling of PSDs was performed for pure PCM and PSDs using USP Apparatus II (Tianjin Guoming Medicinal Equipment Co., Ltd.) [27]. The sink condition of powders was maintained using a dialysis tube. In this method, 900 ml de-mineralized (DM) water was used as dissolution medium, and the paddle speed & temperature were maintained at 50 ± 2 rpm & 37.0˚C ± 0.5˚C, respectively. Briefly, the samples under study (either pure drug or PSDs, equivalent to 27 mg of PCM) were incorporated into a piece of dialysis tubing and placed into the dissolution medium. An aliquot (10 ml) was withdrawn repeatedly at 5, 10, 15, 30, 45, 60, and 120 min followed by replacement with dissolution medium. The samples were filtered and the concentration of PCM at each point was measured as described in the previous section. Three replicates of each sample were carried out and the mean values were calculated followed by plotting against corresponding sampling time to construct the dissolution-time profile.

2.5. Solid-State Characterization of PSDs

2.5.1. Differential Scanning Calorimetry (DSC) and Powder X-Ray Diffraction (PXRD) Study

DSC study was performed to observe the crystallinity of PCM, silica, PEG, Na-citrate, and PSD using a Differential Scanning Calorimeter (Exstar SII DSC7020, Hitachi High-Tech Science Corporation, Tokyo, Japan). In each case, 3 - 5 mg sample was placed in sealed standard aluminum pans and heated from 0˚C - 300˚C, at a scanning rate of 10˚C/min under nitrogen purge keeping an empty aluminum pan as reference [28].

Additionally, an X-ray diffractometer (RAD-C, Rigaka Denki Co. Ltd. Tokyo, Japan) was used for the diffraction study. The PSD, silica, PEG, Na-citrate, and PCM were exposed to Cu-Kα radiation (30 kV and 50 mA) and scanned from 2˚ - 40˚ (2θ) at a scanning rate of 5˚/min [28].

2.5.2. Fourier Transform Infrared Spectroscopy (FTIR) Study

The nature of drug-carriers interaction in PSD was investigated using IR spectra

measured by the diffused reflection method using an FTIR spectrometer (IR-Prestige 21, Shimadzu Co. Japan). A disk of samples was prepared by grounding and thorough mixing with potassium bromide. The scanning range was 400 - 4000 cm^{-1} with resolution 1 cm^{-1} [28].

2.5.3. Scanning Electron Microscopy (SEM) Study

The shape, surface, and cross-sectional morphology of PCM, silica, PEG, Na-citrate, and PSD were observed using a scanning electron microscope (SSX-500, Shimadzu, Japan) after platinum metallization. An accelerating voltage of 15 kV was applied [28].

2.6. Animal Study

Five weeks aged male Swiss albino mice of body weight 28 - 30 gm were collected from the animal house of the Department of Pharmacy, Jahangirnagar University, Savar, Dhaka, Bangladesh. The mice were kept in animal cages under standard environmental conditions (22˚C - 25˚C, 60% - 70% humidity, and 12 hr light/12hr dark cycles). They were acclimated for 2 weeks and fed with standard foods. Throughout the study period, the animals cared for following codex rules and guidelines for research for animal experimentation [29]. The experimental protocol was approved by the Institutional Animal, Medical Ethics, Biosafety, and Biosecurity Committee (IAMEBBC) of the Institute of Biological Sciences, University of Rajshahi, Bangladesh.

2.6.1. Evaluation of Analgesic Activity of PSD

The experimental mice were divided into five groups, each consisting of five animals for treatment protocol (**Table 2**). Age-matched five healthy normal mice were used as normal control (NC). The writhing syndrome was elicited by an intraperitoneal injection of 1% v/v acetic acid at the dose of 0.1 ml/10gm body weight [30]. According to protocol PSD, PCM, and/or vehicle (0.5% methylcellulose) were orally administered to test animals and allowed 30 min for

Table 2. Treatment plan to evaluate analgesic activity.

Mice Group (n = 5)	Dose Administered Orally
NC	Vehicle
PCM30	Vehicle + PCM, 30 mg/kg
PSD10L	Vehicle + Formulation PSD10 eq. to 3 mg/kg PCM
PSD10M	Vehicle + Formulation PSD10, eq. to 30 mg/kg PCM
PSD10H	Vehicle + Formulation PSD10, eq. to 300 mg/kg PCM
NC	Vehicle

NC (normal control), mice received vehicle only; PCM30, mice received paracetamol 30 mg/kg; PSD10L, mice received PSD10 equivalent to 3 mg/kg of paracetamol (low dose); PSD10M, mice received PSD10 equivalent to 30 mg/kg of paracetamol (medium dose); PSD10H, mice received PSD10 equivalent to 300 mg/kg of paracetamol (high dose).

systemic absorption of the drug. After that acetic acid was administered through intraperitoneal injection to each group and the total number of writhing movements was counted to 30 min.

2.6.2. Evaluation of Effect of PSD on Hepatocytes

Like evaluation of analgesic activity, age-matched healthy normal mice were also divided into five groups for evaluation of the influence of PSD10 on hepatocytes, and the treatment protocol was designed as in Table 3. According to the protocol pure PCM and PSD at 300 mg/kg dose (acute toxic dose) along with vehicle (0.5% methylcellulose) were orally administered into mice [31]. Following 24 hours of administration, the mice were anaesthetized with diethyl ether and sacrificed by cervical decapitation. Blood was collected directly from the heart by syringe for analysis of liver biomarkers e.g., serum glutamic oxaloacetic transaminase (SGOT) and serum glutamic pyruvic transaminase (SGPT), and alkaline phosphatase (ALP). However, the blood samples were centrifuged at 4000 rpm for 10 min (Centurion, UK) using Na-EDTA as an anti-coagulant. The supernatant serum was then collected to estimate SGOT, SGPT, and ALP using commercial kits.

In histology study, liver from each group was collected and fixed in phosphate-buffered saline containing 10% v/v formalin. The tissues were washed in running tap water, dehydrated in descending grades of isopropanol, and finally cleaned with xylene. After embedding in paraffin wax, several transverse sections (5 μm) were cut from the mid-organ level with a microtome and stained with hematoxylin-eosin (HE). The specimens were observed under a light microscope (Olympus IX71) and photographs were taken with a digital camera.

2.7. Stability Study of PSD10

An accelerated stability study of this optimized formulation (PSD10) was conducted according to the guidelines of International Conference Harmonization (ICH) Topic Q1A (R2) Stability Testing of new Drug Substances and Products [32] and WHO Technical Report Series, No. 863, 1996 Annex 5 [33]. Briefly, quantity of freshly prepared sample was taken in six amber glass bottles, sealed with aluminium cork and stored in a stability chamber (Newtronic Nec216R10SI, Newtronic Lifecare Equipment Pvt Ltd., India) maintaining 40˚C ± 2˚C temperature & 75% ± 5% RH.

Table 3.Treatment plan for hepatic toxicity study.

Mice Group (n = 5)	Dose Administered Orally
NC	Vehicle
PCM300	Vehicle + PCM, 300 mg/kg
PSD10H	Vehicle + Formulation PSD10, eq. to 300 mg/kg PCM

NC (normal control), mice received vehicle only; PCM300, mice received paracetamol 300 mg/kg; PSD10H, mice received PSD10 equivalent to 300 mg/kg of paracetamol.

EE and dissolution study was performed according to Section 2.3 and 2.4, respectively at 0 month (initial), and after 3 and 6 months (Table 4). Physicochemical characterization for re-crystalline behaviour of PCM in PSD10 was evaluated by DSC and PXRD study at the end of stability period.

2.8. Statistical Analysis

Results were expressed as mean ± S.E.M. Statistical analyses were performed using Student's t-test. The value of $p < 0.05$ indicates statistically significance.

3. Results

3.1. Encapsulation Efficiency (EE) of PSDs

The EE values of PSDs are presented in Table 5. Silica as a carrier offered (Group-1) more than 90% w/w EE that exploring silica has good adsorption efficiency. But there was no significant difference within this group and hence, PSD1 comprising the lowest concentration of silica was privileged to proceed for consecutive development. However, PEG at different ratios were added to PSD1 resulting in reduced EE (88.57% w/w) in PSD4 and was maximized to more than 92% w/w in PSD5 & PSD6. There was no significant difference considering the EE value of PSD5 & PSD6, and therefore, PSD5 with a lower concentration of PEG was a fastidious formulation. Again, the effect of Na-citrate along with PSD1 explored decreased EE value 82.07% w/w at the lowest concentration in

Table 4. Accelerated stability study protocol of PSD10.

Formulation	Storage Condition	Time Periods (Months)	Denoted as
PSD10	40˚C ± 2˚C and 75% ± 5% RH	0 (initial)	PSD10St0
		3	PSD10St3
		6	PSD10St6

Table 5. Percentage of yield and encapsulation efficiency (%) of PSDs.

Group	Formulations	Encapsulation Efficiency (% w/w)
1	PSD1	91.09 ± 0.60
	PSD2	90.37 ± 1.04
	PSD3	91.83 ± 1.17
2	PSD4	88.57 ± 0.92
	PSD5	92.66 ± 1.10
	PSD6	92.33 ± 1.45
3	PSD7	82.07 ± 0.64
	PSD8	92.94 ± 0.61
	PSD9	91.00 ± 1.53
Optimized	PSD10	94.39 ± 0.67

PSD7. At moderately higher concentration, EE was significantly ($p < 0.001$) improved to 92.94% w/w when an equal ratio of PCM, silica, PEG, and Na-citrate used in PSD8. Finally, EE was further maximized to 94.39% w/w by using the optimized concentration of silica, PEG, Na-citrate to get the formulation PSD10.

3.2. *In-Vitro* Dissolution Profiling

3.2.1. Optimization of Concentration of Silica

Dissolution profiles of PSDs containing PCM and silica at different ratios are depicted in Figure 2(a). Drug release from PSD1, PSD2, and PSD3 (Group-1) were significantly higher ($p < 0.001$) than from pure PCM at each sampling point throughout the study. Within this group, higher drug release by PSD1 was with a level of significance $p < 0.05$ than PSD2 up to 30 min and $p < 0.001$ & $p < 0.05$ than PSD3 up to 45 & 120 min, respectively. Hence, the optimum ratio of PCM and silica was 1:1.

3.2.2. Optimization of Concentration of PEG with PSD1

The drug release profiles are presented in Figure 2(b). The increment of drug releases from Group-2 was highly significant ($p < 0.001$) than pure PCM at each sampling time point. In this group, both PSD5 & PSD6 showed significantly higher ($p < 0.05$) release than PSD4 up to 45 min. Between PSD5 & PSD6, the

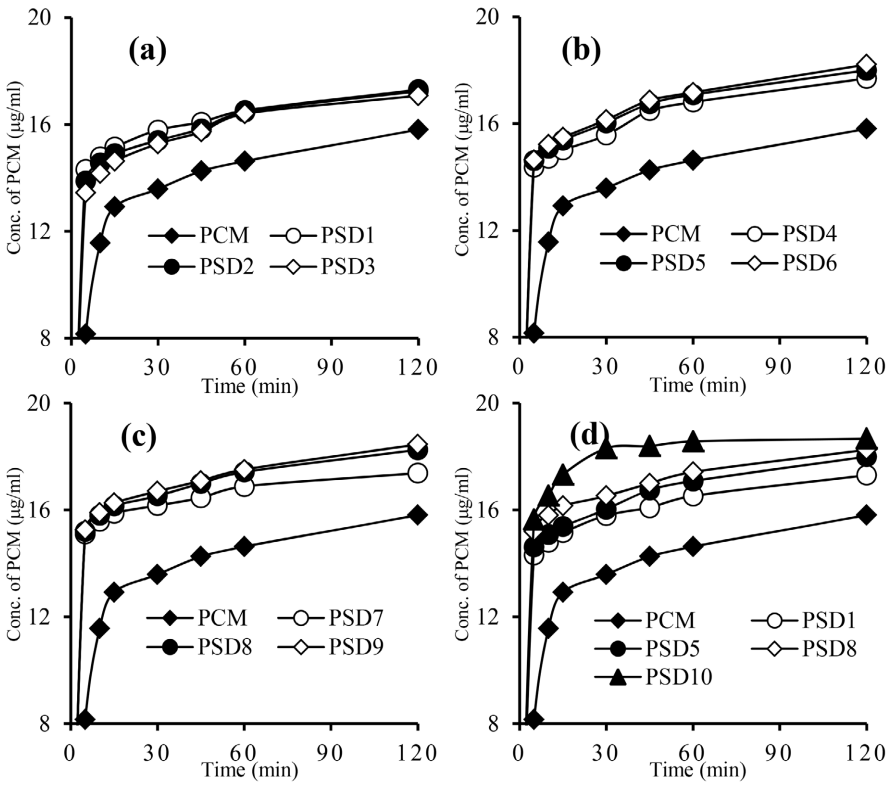

Figure 2. Dissolution profile; (a) PCM, PSD3, PSD2 and PSD1 (b) PCM, PSD4, PSD5 and PSD6 (c) PCM, PSD7, PSD8 and PSD9 (d) to optimize the appropriate concentration of the excipients PCM, PSD1, PSD5, PSD8 and PSD10. Each value represents mean ± SEM (n = 3).

release quantity at each point was too closer that there were no significant differences. As PSD5 contains PEG at a quantity by half as of PSD6, therefore, PSD5 can be privileged as the optimum formulation. Beside this, the drug release from PSD5 was also significantly higher ($p < 0.01$) than PSD1.

3.2.3. Optimization of Concentration of Na-Citrate with PSD1

Dissolution profiles were compared among each other and with pure PCM and PSD1 (**Figure 2(c)**). *In-vitro* drug releases were significantly increased ($p < 0.001$) by group-3 formulations than pure PCM at each sampling time point. Within this group, PSD8 & PSD9 had significantly higher drug release ($p < 0.05$) than PSD7 after 30 min. Like group-2, PSD8, and PSD9 with Na-citrate at various ratios could show no significant difference in drug release. Therefore, the concentration of Na-citrate used in PSD8 was selected as optimum.

3.2.4. Dissolution Characteristic of PSD with Optimized Concentration of Silica, PEG and Na-Citrate

A solid dispersion formulation (PSD10) was formulated using the optimized concentration of silica, PEG, and Na-citrate, and its dissolution profile was compared with that of pure PCM, optimized PSD1, PSD5, and PSD8 (**Figure 2(d)**). *In-vitro* drug release was maximum and highly significant ($p < 0.001$) by PSD10 than that of pure PCM, PSD1, PSD5 and PSD8 at each sampling time point and maximum steady concentration (**Figure 2(d)**) at 30 min, meanwhile PSD1, PSD5 and PSD8 consumed more time (>60 min) to reach the steady level.

Therefore, depending on EE and *in-vitro* drug release profile PSD10 was designated as a proficient formulation, and thereafter its solid-state characterization, evaluation of analgesic efficacy, as well as hepatotoxicity study was carried out.

3.3. Solid-State Characterization

3.3.1. Crystallinity Analysis by DSC and PXRD

DSC thermograms of PCM, silica, PEG, Na-citrate, and PSD10 are shown in **Figure 3**. The thermogram of PCM showed an endothermic peak at 175.04˚C implying the crystalline nature. PEG and Na-citrate also produced a sharp endothermic peak at 61.86˚C and 165.05˚C, respectively. But silica had no sharp peak rather a broad peak at 92.87˚C indicating no crystalline property. The thermogram of PSD10 contains peaks with low intensity at 47.57˚C corresponding to the shifted peaks of PEG. The broadening of an endothermic peak at 168.32˚C is probably connected with the peak of pure PCM towards lower temperature values indicating the conversion of PCM from crystalline to amorphous form.

PXRD patterns of PCM, silica, PEG, Na-citrate, and PSD10 are shown in **Figure 4**. Sharp peaks were observed at 2θ angles of 12.94˚, 15.62˚, 18.33˚, 23.57˚, 29.93˚, 24.46˚, and 29.11˚ for PCM. Similarly, peaks were found at 19.33 and 23.59˚ for PEG and 11.66˚, 17.92˚, 22.70˚, 25.52˚, 30.42˚, 34.14˚, and 37.07˚ for Na-citrate. But no sharp peak was observed for silica due to its amorphous nature. In the case of PSD10, no sharp peak for crystallinity was observed as in

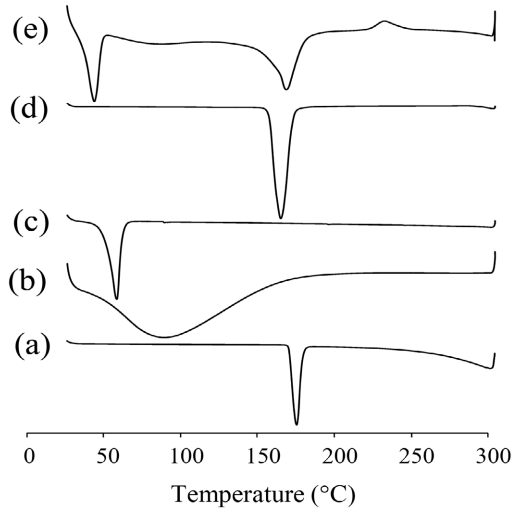

Figure 3. DSC thermograms of (a) pure PCM (b) Silica (c) PEG (d) Na-citrate (e) PSD10.

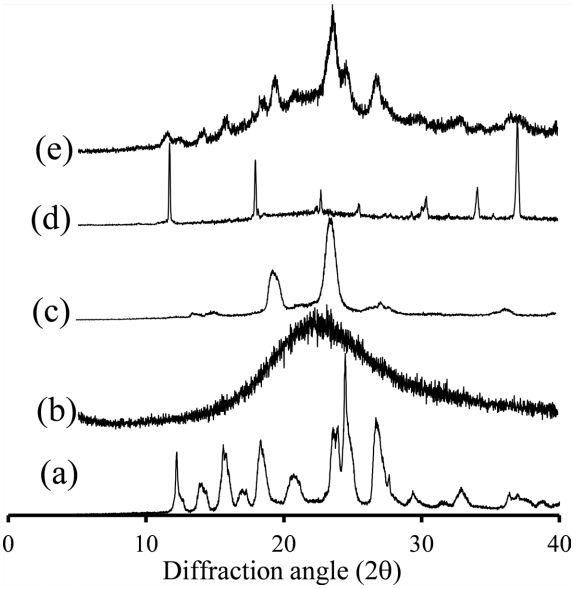

Figure 4. Powder X-ray diffraction patterns of (a) pure PCM (b) Silica (c) PEG (d) Na-citrate (e) PSD10.

pure PCM and the amplitude of the diffraction peaks suggested that the degree of crystallinity of PCM in PSD10 is almost disappeared indicating that, a polymorphic transformation of PCM might have occurred during the formulation of PSD10 resulting an amorphous state.

3.3.2. Interaction Study by FTIR

The interaction among pure PCM, silica, PEG, and Na-citrate was examined by FTIR spectroscopy. The results of FTIR spectroscopy of PCM, silica, PEG, Na-citrate, and PSD10 are shown in **Figure 5**. PCM showed bands at 3319 and 1651 cm^{-1} due to stretching by amine (-NH-) and carbonyl (=CO) groups, respectively. A bending vibration for the amide group was observed at 1562 cm^{-1} [34]. Silica showed band at 1055 cm^{-1} due to the deformation of the -OH group

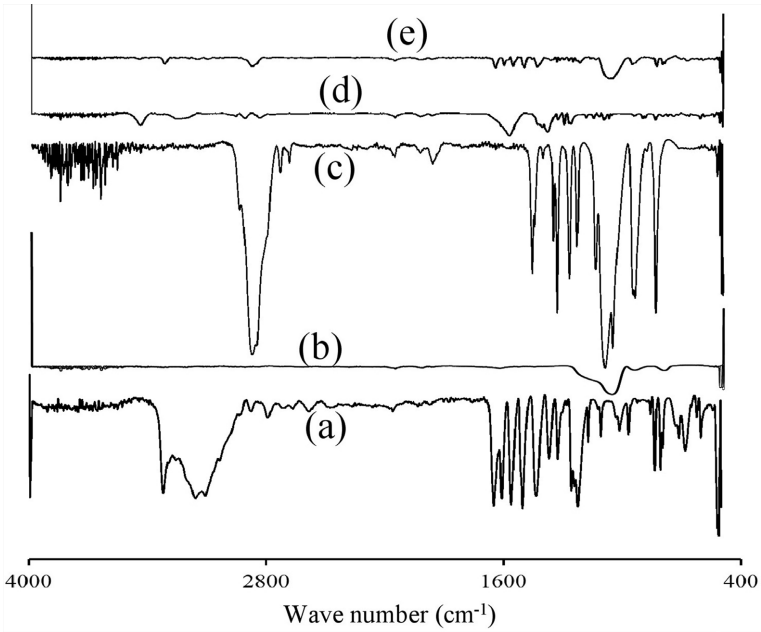

Figure 5. FTIR spectra of (a) pure PCM (b) Silica (c) PEG (d) Na-citrate (e) PSD10.

of Si-OH and a sharp decrease in the intensity of the Si-OH band at 950 cm^{-1} [35]. PEG showed bands at 2885, 1340, 1278, and 1093 cm^{-1} for C-H stretching, C-H bending, C-O-H stretching and O-H stretching, respectively [36]. Accordingly, Na-citrate generated bands at 3448, 2920 & 2846, 1579, 1378 and 1303 and 1271 cm^{-1} due to O-H stretching, -CH_2- stretching, COO- oscillation, deformation mode of -CH_2- stretching, and oscillation of -COOH group, respectively [37]. However, the intensity of the band for stretching of carbonyl group as in PCM was reduced and the band due to stretching and bending of -NH- was disappeared in FTIR spectra of PSD10. This might be due to the possible interaction between the amide group of PCM with C-O-H of PEG and with -COOH of Na-citrate. The band for Si-OH group of silica found at 1093 cm^{-1} was shifted to 1076 cm^{-1} in PSD10 possibly due to chemisorption of the conjugate through -OH group of PEG. Thus, FTIR spectra of PSD10 revealed that there was no incompatible interaction between PCM and the compositions.

3.3.3. Morphological Study by SEM

The SEM images of the PCM, silica, PEG, Na-citrate, and PSD10 are shown in **Figure 6**. The micrograph of PCM exhibited the presence of needle-shaped crystals with a significant number of brittle powders (**Figure 6(a)**). The SEM images (**Figure 6**) of silica, PEG and Na-citrate exhibited amorphous powder, irregularly shaped crystal, and regular cubic crystal, respectively. But the image of PSD10 (**Figure 6(e)**) showed no existence of crystal of PCM except the possible cubes of Na-citrate onto which other ingredients used in formulation were molecularly deposited demonstrating the possible conversion of PCM crystals to amorphous form through chemical interaction as also indicated by FTIR study. However, the surface morphology of PSD10 might be expressed as an amor-

phous form identical to that of silica (Figure 6). The probable reason for this identical morphology might be due to an adsorption mechanism of the coalescent formed through interaction among the PCM, PEG- and Na-citrate on to silica surface.

3.4. Analgesic Activity of PSD10

The result obtained from the writhing test in mice was illustrated in Figure 7. The average writhing number for NC, PCM30, PSD10L, PSD10M, and PSD10H mice groups were 50, 32.75, 46.50, 22.73 and 5.75, respectively. Among the treatment group, a significant reduction in writhing number by PSD10M ($p < 0.05$) and PSD10H mice ($p < 0.001$) was observed than PCM30 mice. It is noticeable that at a similar dose, the formulation PSD10 showed 1.44-fold writhing

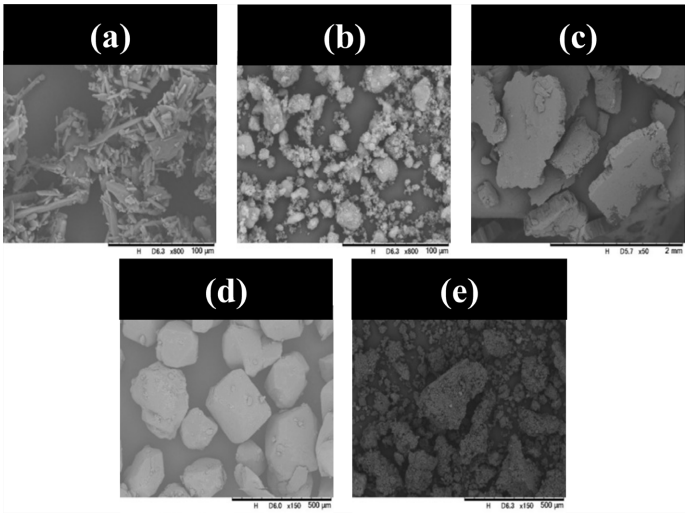

Figure 6. SEM images of (a) pure PCM (b) Silica (c) PEG (d) Na-citrate (e) PSD10.

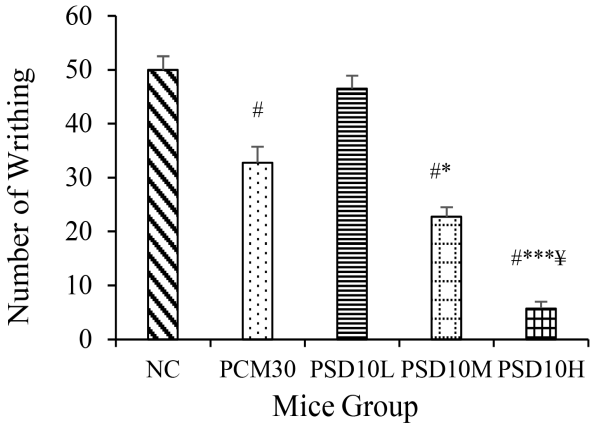

Figure 7. Comparative of analgesic efficacy of pure PCM and PSD10 explored with change in number of writhing in mice of different groups. Results are presented as mean ± S.E.M. (n = 5); #p < 0.001 vs. NC; *p < 0.05, **p < 0.01, ***p < 0.001 vs. PCM30; ¥p < 0.001 vs. PSD10M. NC mice received vehicles only; PCM30 mice received 30 mg/kg pure paracetamol; PSD10L, PSD10M & PSD10H mice groups received the formulation at dose 3, 30 & 300 mg/kg paracetamol, respectively.

inhibition ability than pure PCM (PCM30). Additionally, at 10 times higher dose (PSD10H) it was 5.69-fold greater than the same, indicating PSD10 with better analgesic efficacy in contrast to pure PCM.

3.5. Hepatoprotective Activity of PSD10

An acute toxic dose (300 mg/kg body weight) was applied to mice to observe the toxicity and survival rate. None of the mice died in NC, PCM300, and PSD10H groups after 24 hours of treatment (Table 6).

After 24 hours of administration with pure PCM and PSD10 at dose 300 mg/kg body weight, the levels of SGPT, SGOT, and ALP in PCM300 mice were found to be significantly increased by 1.9, 1.75 and 1.71-fold, respectively in contrast to NC mice. But in PSD10 mice the level of SGPT, SGOT, and ALP was reduced by 1.8, 1.54, and 1.67-fold, respectively in contrast with PCM300 mice, which are also analogous with the values of NC mice (Figure 8).

In addition, the microphotograph (Figure 9) of a thin section of the liver of NC mice represents intact hepatocytes with normal cellular architecture. Liver tissue obtained from PCM300 mice showed higher cellular necrosis compared to that of PSD10H mice, although both the groups were treated with the same PCM dose (300 mg/kg body weight). However, the cellular architecture of PSD10H

Table 6. Survival rate of mice after 24 hours treatment with PCM and PSD10.

Mice Groups (n = 5)	Total mice	Survivals	Deaths	Survival rate (%)
NC	5	5	0	100
PCM300	5	5	0	100
PSD10H	5	5	0	100

NC (normal control), mice received vehicle only; PCM300, mice received paracetamol 300 mg/kg; PSD10H, mice received PSD10 equivalent to 300 mg/kg of paracetamol.

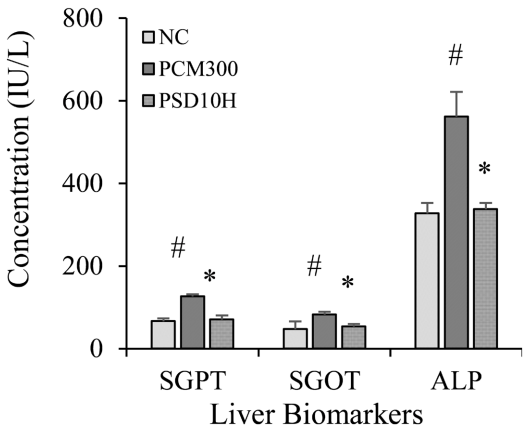

Figure 8. Changes in liver biomarker (SGPT, SGOT and ALP) levels demonstrating hepatic toxicity quantitatively induced by pure PCM and PSD10. Results are presented as the mean ± S.E.M. (n = 5); $^{\#}p < 0.05$ vs. NC (increased); $^{*}p < 0.05$ vs. PCM300 (reduced). NC mice received vehicles only; PCM300 mice received 300 mg/kg pure paracetamol; PSD10H mice received formulation equivalent to 300 mg/kg paracetamol.

mice was comparable with that of NC mice which gave evidence of very negligible damage of hepatocytes with the new formulation, which might also be authenticated by the corresponding SGPT, SGOT, and ALP values in contrast to the NC group.

3.6. Stability Study of PSD10

3.6.1. Encapsulation Efficiency (EE) of PSD10 under Stability Conditions

The EE of PSD10 under designed stability conditions are presented in Table 7. EE of PSD10St0 (Initial), PSD10St3 and PSD10St6 are 94.05%, 93.51% and 93.35%, respectively. However, no significant ($p < 0.05$) changes were found in EE of stability samples compared to freshly prepared PSD10 (Initial).

3.6.2. Dissolution Characteristic of PSD10 under Stability Conditions

Dissolution profile of PSD10St0 (Initial), PSD10St3 and PSD10St6 are shown in Figure 10. Although inconsequential change in the data was found, but it revealed that *in-vitro* release pattern of the PCM from PSD10 was not altered significantly ($p < 0.05$) under designed stability protocol.

3.6.3. Crystallinity Analysis by DSC and PXRD of PSD10 under Stability Conditions

DSC thermograms of stability samples (PSD10St3 and PSD10St6) showed identical endothermic peaks as of PSD10St0 (Figure 11) considering the shape and

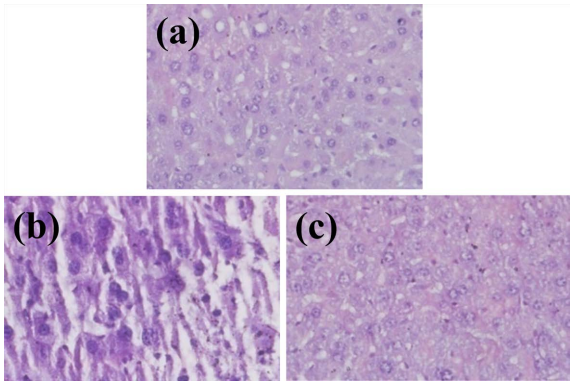

Figure 9. Representative microphotographs (×400) exploring the effect of pure PCM and PSD10 on liver at acute toxic dose.(a) NC mice received vehicles only; (b) PCM300 mice groups received pure paracetamol at dose 300 mg/kg; (c) PSD10H groups received formulation equivalent to 300 mg/kg paracetamol.

Table 7. Percentage of yield and encapsulation efficiency (%) of PSD10 under stability conditions.

Formulations	EE (% w/w)	% Change of EE
PSD10 (Initial)	94.05 ± 0.39	-
PSD10St3	93.51 ± 0.32	−0.574
PSD10St6	93.35 ± 0.33	−0.744

Results are presented as the mean ± S.E.M (n = 3). *$p < 0.05$, vs PSD10 (Initial).

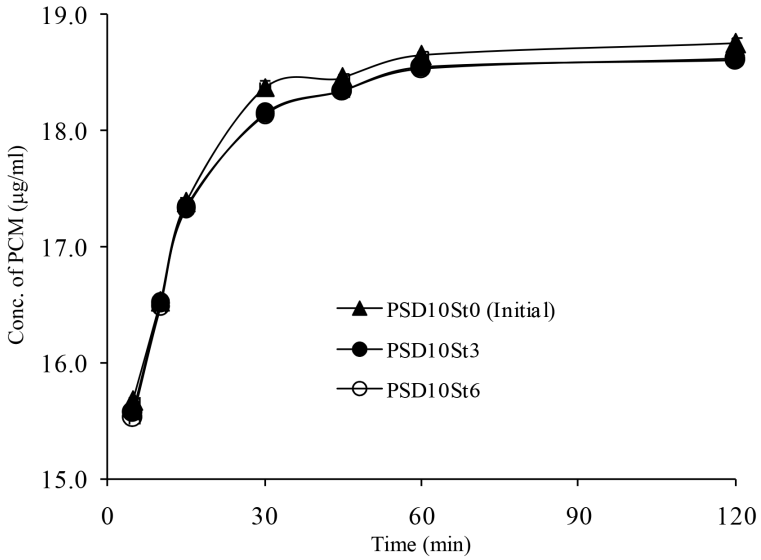

Figure 10. Dissolution profiles of PSD10St0 (Initial), PSD10St3 and PSD10St6. Each value represents mean ± SEM (n = 3).

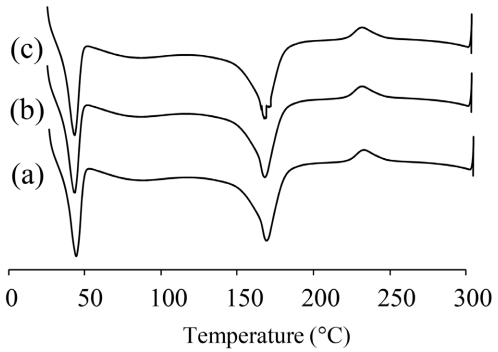

Figure 11. DSC thermograms of (a) PSD10St0 (Initial), (b) PSD10St3, and (c) PSD10St6.

position. However, the endothermic peaks of PSD10St3 at 47.97˚C for PEG and at 168.56˚C for Na-citrate are indistinguishable with that of PSD10. Similarly, PSD10St6 showed peaks with low intensity at 47.97˚C for PEG and at 167.80˚C for Na-citrate which alike with that of PSD10 also.

In addition, PXRD patterns of PSD10St3 and PSD10St6 (**Figure 12**) showed no new or unusual peak caused for any re-crystalline processes. These diffractograms are closely similar to that of PSD10 of initial study.

4. Discussion

With an apparition to increase analgesic activity with circumventing hepatic damage a new formulation PSD10, possessing the highest EE (**Table 5**) was developed using the combination of optimized concentration of silica, PEG, and Na-citrate. The dissolution of PCM could be significantly maximized with this newly developed formulation (**Figure 2(d)**) due to the adsorbing of PCM molecules onto the silica surface that was reported by Ghosh *et al.* previously and increased hydrophilicity by the presence of PEG and Na-citrate [38] [39] [40]. Due

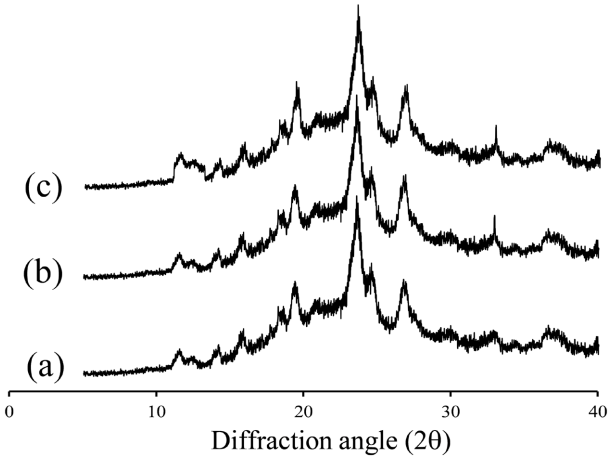

Figure 12. Powder X-ray diffraction patterns of (a) PSD10St0 (Initial),(b) PSD10St3, and (c) PSD10St6.

to the combined effect of carriers in PSD10 drug release was very fast at 5 min and picked the concentration within 30 min. Collectively, the solid-state characterization indicated that the crystalline behaviour of PCM was mostly devastated using the combination of PCM, PEG, and Na-citrate. The higher dissolution of PSD10 might be a possible conversion of crystal nature of PCM and chemisorption on silica, increased wettability by PEG, and hydrotropic solubilizing effect of Na-citrate.

To study analgesic efficacy along with the influence on hepatocytes *in-vivo*, the mice model was selected because NAPQI-mediated hepatic damage is more pronounced in mice over the rat and this model was extensively used [41] [42]. However, PCM as a COX-2 selective inhibitor and centrally acting analgesic possess the ability to reduce writhing [3] [4]. In the acetic acid-induced writhing test PSD10 showed a significant decrease in the number of writhing by 1.44-fold greater compared to pure PCM at an equal dose (30 mg/kg). This result indicated that fast dissolution and subsequent rapid absorption of PCM occurred in GIT from the solid dispersion formulation (PSD10) as previously reported by various authors [43] [44] [45].

The effect of PSD10 in mice hepatocytes was evaluated with the biomarkers (SGPT, SGOT, and ALP) and histology of the liver. After 24 hours of administration, in contrast to NC mice, pure PCM abruptly raised SGOT, SGPT, and ALP concentrations significantly. But in the mice groups administered with PSD10 at an equal dose, these parameters were found close to NC mice. In addition, the histological study demonstrated that comparatively negligible hepatocellular necrosis occurred in PSD10 mice compare with PCM mice administered with equal doses. This result authenticated that rapid absorption of PCM from GIT with PSD10 improving analgesic potential and the altered effect of PSD10 on liver metabolism might be comparable to the outcome of PCM nanoparticles [12].

The amorphous paracetamol in a dosage form was reported to lead an unde-

sired crystallization during its shelf life [46] [47]. Hence, the stability testing of such formulation is essential. In consequence of this study, the EE values of PSD10St3 and PSD10St6 stored for 3 and 6 months respectively showed no significant percentage changes of PCM encapsulation efficiency (**Table 7**) and complied with the limit (5%) of STABILITY TESTING OF NEW DRUG SUBSTANCES AND PRODUCTS Q1A (R2) guidelines [32]. The comparative *in-vitro* dissolution study among PSD10St3 and PSD10St6 with PSD10St0 showed no significant deterioration of drug release as well that nullified the possibility of PCM re-crystallization upon storage at accelerated stability condition. Similar observation was reported by Lehmkeper *et al.* (2017) that the impact of relative humidity (RH) is insignificant on the solubility of paracetamol dispersed in polymers [48]. Finally, the re-crystalline nature of PCM10 after stability storage was verified by comparing the DSC and PXRD data of the initial and stability samples and found no new endothermic and diffraction peak in PSD10St3 and PSD10St6 demonstrating PCM's stability and compatibility in formulation with the carriers used.

5. Conclusion

Paracetamol loaded in solid dispersion containing silica, PEG and Na-citrate have been successfully proved in enhancing *in-vitro* dissolution, *in-vivo* analgesic efficacy along with chemical and physical stability. At the same time, it exerts a significant hepatoprotective property compared to pure paracetamol. Being a simple and inexpensive drug delivery approach, the established solid dispersion formulation can be compared in parallel to any modern techniques like nano-formulations. Hence, this newer formulation of paracetamol would be a competent alternative to improve the analgesic and hepatoprotective properties in the drug delivery era. To depict the absorption behaviour and/or altered mechanism of liver metabolism of PCM loaded in PSD10 pharmacokinetic study may be proposed as a future direction.

Acknowledgements

The authors acknowledge the Department of Pharmaceutical Engineering, School of Pharmaceutical Sciences, University of Shizuoka, Shizuoka, Japan for DSC, PXRD, FTIR and SEM analysis.

Ethical Clearance

The animal experiment in our study was conducted according to the guidelines of the Institutional Animal, Medical Ethics, Biosafety and Biosecurity Committee (IAMEBBC) at the Institute of Biological Sciences, University of Rajshahi, Bangladesh (Memo number: 473(18)/320/IAMEBBC/IBSC).

Conflicts of Interest

The authors declare no conflicts of interest regarding the publication of this paper.

References

[1] PubChem—Open Chemistry Database (2018) Paracetamol. https://pubchem.ncbi.nlm.nih.gov/compound/acetaminophen

[2] Graham, G.G., Davies, M.J., Day, R.O., Mohamudally, A. and Scott, K.F. (2013) The Modern Pharmacology of Paracetamol: Therapeutic Actions, Mechanism of Action, Metabolism, Toxicity and Recent Pharmacological Findings. *Inflammopharmacology*, **21**, 201-232. https://doi.org/10.1007/s10787-013-0172-x

[3] Illangakoon, U.E., Gill, H., Shearman, G.C., Parhizkar, M., Mahalingam, S., Chatterton, N.P. and Williams, G.R. (2014) Fast Dissolving Paracetamol/Caffeine Nanofibers Prepared by Electrospinning. *International Journal of Pharmaceutics*, **477**, 369-379. https://doi.org/10.1016/j.ijpharm.2014.10.036

[4] Sharma, C.V. and Mehta, V. (2014) Paracetamol: Mechanisms and Updates. *Continuing Education in Anaesthesia Critical Care & Pain*, **14**, 153-158. https://doi.org/10.1093/bjaceaccp/mkt049

[5] Granberg, R.A. and Rasmuson, A.C. (1993) Solubility of Paracetamol in Pure Solvents. *Journal of Chemical & Engineering Data*, **44**, 1391-1395. https://doi.org/10.1021/je990124v

[6] Gaisford, S. and Saunders, M. (2012) Essentials of Pharmaceutical Preformulation. John Wiley & Sons, West Sussex. https://doi.org/10.1002/9781118423226

[7] Forrest, J.A.H., Clements, J.A. and Prescott, L.F. (1982) Clinical Pharmacokinetics of Paracetamol. *Clinical Pharmacokinetics*, **7**, 93-107. https://doi.org/10.2165/00003088-198207020-00001

[8] Hinson, J.A., Pohl, L.R., Monks, T.J. and Gillette, J.R. (1981) Acetaminophen-Induced Hepatotoxicity. *Life Sciences*, **29**, 107-116. https://doi.org/10.1016/0024-3205(81)90278-2

[9] James, L.P., Mayeux, P.R. and Hinson, J.A. (2003) Acetaminophen-Induced Hepatotoxicity. *Drug Metabolism and Disposition*, **31**, 1499-1506. https://doi.org/10.1124/dmd.31.12.1499

[10] Yoon, E., Babar, A., Choudhary, M., Kutner, M. and Pyrsopoulos, N. (2016) Acetaminophen-Induced Hepatotoxicity: A Comprehensive Update. *Journal of Clinical and Translational Hepatology*, **4**, 131-142. https://doi.org/10.14218/JCTH.2015.00052

[11] Lee, W.M. (2017) Acetaminophen (APAP) Hepatotoxicity—Isn't It Time for APAP to Go Away? *Journal of Hepatology*, **67**, 1324-1331. https://doi.org/10.1016/j.jhep.2017.07.005

[12] Biazar, E., Rezayat, S.M., Montazeri, N., Pourshamsian, K., Zeinali, R., Asefnejad, A., Rahimi, M., Zadehzare, M., Mahmoudi, M., Mazinani, R. and Ziaei, M. (2010) The Effect of Acetaminophen Nanoparticles on Liver Toxicity in a Rat Model. *International Journal of Nanomedicine*, **5**, 197-201. https://doi.org/10.2147/IJN.S5894

[13] Yang, F., Medik, Y., Li, L., Tian, X., Fu, D., Brouwer, K.I., Wagner, K., Sun, B., Sendi, H., Mi, Y. and Wang, A.Z. (2020) Nanoparticle Drug Delivery Can Reduce the Hepatotoxicity of Therapeutic Cargo. *Small*, **16**, e1906360. https://doi.org/10.1002/smll.201906360

[14] Ebrahimi, A., Saffari, M., Dehghani, F. and Langrish, T. (2016) Incorporation of Acetaminophen as an Active Pharmaceutical Ingredient into Porous Lactose. *International Journal of Pharmaceutics*, **499**, 217-227. https://doi.org/10.1016/j.ijpharm.2016.01.007

[15] Lloyd, G.R., Craig, D.Q.M. and Smith, A. (1999) A Calorimetric Investigation into

the Interaction between Paracetamol and Polyethlene Glycol 4000 in Physical Mixes and Solid Dispersions. *European Journal of Pharmaceutics and Biopharmaceutics*, **48**, 59-65. https://doi.org/10.1016/S0939-6411(99)00022-3

[16] Gryczke, S., Qi, A., Belton, P. and Craig, D.Q.M. (2008) Characterization of Solid Dispersions of Paracetamol and Eudragit® Prepared by Hot-Melt Extrusion Using Thermal, Microthermal and Spectroscopic Analysis. *International Journal of Pharmaceuti*, **354**, 158-167. https://doi.org/10.1016/j.ijpharm.2007.11.048

[17] Sahoo, C.K., Satyanarayana, K. and Ramana, D.V. (2017) Formulation and Evaluation of Solid Dispersion Containing Paracetamol. *International Journal of Pharmaceutical and Clinical Research*, **3**, 722-726.

[18] Singh, A., Sharma, P.K., Meher, J.G. and Malviya, R. (2011) Evaluation of Enhancement of Solubility of Paracetamol by Solid Dispersion Technique Using Different Polymers Concentration. *Asian Journal of Pharmaceutical and Clinical Research*, **4**, 117-119.

[19] Kaialy, W., Larhrib, H., Chikwanha, B., Shojaee, S. and Nokhodchi, A. (2014) An approach to Engineer Paracetamol Crystals by Antisolvent Crystallization Technique in Presence of Various Additives for Direct Compression. *International Journal of Pharmaceutics*, **464**, 53-64. https://doi.org/10.1016/j.ijpharm.2014.01.026

[20] Al-Hamidi, H., Edwards, A.A., Mohammad, M.A. and Nokhodchi, A. (2010) To Enhance Dissolution Rate of Poorly Water-Soluble Drugs: Glucosamine Hydrochloride as a Potential Carrier in Solid Dispersion Formulations. *Colloids and Surfaces B: Biointerfaces*, **76**, 170-178. https://doi.org/10.1016/j.colsurfb.2009.10.030

[21] Bhusnure, O.G., Kazi, P.A., Gholve, S.B., Ansari, M.M.A.W. and Kazi, S.N. (2014) Solid Dispersion: An Ever Green Method for Solubility Enhancement of Poorly Water Soluble Drugs. *International Journal of Research in Pharmacy and Chemistry*, **4**, 906-918.

[22] Sareen, S., Joseph, L. and Mathew, G. (2012) Improvement in Solubility of Poor Water-Soluble Drugs by Solid Dispersion. *International Journal of Pharmaceutical Investigation*, **2**, 12-17. https://doi.org/10.4103/2230-973X.96921

[23] Sridhar, I., Doshi, A., Joshi, B., Wankhede, V. and Doshi, J. (2013) Solid Dispersions: An Approach to Enhance Solubility of Poorly Water Soluble Drug. *Journal of Scientific and Innovative Research*, **2**, 685-694.

[24] Thenmozhi, K. and Yoo, Y.J. (2017) Enhanced Solubility of Piperine Using Hydrophilic Carrier-Based Potent Solid Dispersion Systems. *Drug Development and Industrial Pharmacy*, **43**, 1501-1509. https://doi.org/10.1080/03639045.2017.1321658

[25] Huang, Y. and Dai, W.G. (2017) Fundamental Aspects of Solid Dispersion Technology for Poorly Soluble Drugs. *Acta Pharmaceutica Sinica B*, **4**, 18-25. https://doi.org/10.1016/j.apsb.2013.11.001

[26] Mouffok, M., Mesli, A., Abdelmalek, I. and Gontier, E. (2016) Effect of the Formulation Parameters on the Encapsulation Efficiency and Release Behavior of p-Aminobenzoic Acid-Loaded Ethylcellulose Microspheres. *Journal of the Serbian Chemical Society*, **81**, 1183-1198. https://doi.org/10.2298/JSC160308068M

[27] Mauger, J., Ballard, J., Brockson, R., De, S., Gray, V. and Robinson, D. (2003) Intrinsic Dissolution Performance Testing of the USP Dissolution Apparatus 2 (Rotating Paddle) Using Modified Salicylic Acid Calibrator Tablets: Proof of Principle. *Dissolution Technologies*, **10**, 6-15. https://doi.org/10.14227/DT100303P6

[28] Barman, R.K., Iwao, Y., Funakoshi, Y., Ranneh, A.H., Noguchi, S., Wahed, M.I.I. and Itai, S. (2014) Development of Highly Stable Nifedipine Solid-Lipid Nanoparticles. *Chemical and Pharmaceutical Bulletin*, **62**, 399-406.

https://doi.org/10.1248/cpb.c13-00684

[29] (2019) Codex Rules and Guidelines for Research: Animal Research. https://www.codex.uu.se/?languageId=1

[30] Gawade, S.P. (2014) Acetic Acid Induced Painful Endogenous Infliction in Writhing Test on Mice. *Journal of Pharmacology and Pharmacotherapeutics*, **3**, 348.

[31] Kane, A.E., Mitchell, S.J., Mach, J., Huizer-Pajkos, A., McKenzie, C., Jones, B., Cogger V., Le Couteur, D.G., de Cabo, R. and Hilmer, S.N. (2016) Acetaminophen Hepatotoxicity in Mice: Effect of Age, Frailty and Exposure Type. *Experimental Gerontolog*, **73**, 95-106. https://doi.org/10.1016/j.exger.2015.11.013

[32] (2021) Stability Testing of New Drug Substances and Products Q1A (R2). https://database.ich.org/sites/default/files/Q1A%28R2%29%20Guideline.pdf

[33] (2021) WHO Technical Report Series, No. 863, 1996. https://www.paho.org/hq/dmdocuments/2008/6_Annex_5_report_34.pdf

[34] Takahashi, H., Chen, R., Okamoto, H. and Danjo, K. (2005) Acetaminophen Particle Design Using Chitosan and a Spray-Drying Technique. *Chemical and Pharmaceutical Bulletin*, **53**, 37-41. https://doi.org/10.1248/cpb.53.37

[35] Meyer, B. and Stroyer-Hansen, T. (1972) Infrared Spectra of S4. *The Journal of Physical Chemistry A*, **6**, 3968-3969. https://doi.org/10.1021/j100670a013

[36] Shameli, K., Ahmad, M.B., Jazayeri, S.D., Sedaghat, S., Shabanzadeh, P., Jahangirian, H., Mahdavi, M. and Abdollahi, Y. (2012) Synthesis and Characterization of Polyethylene Glycol Mediated Silver Nanoparticles by the Green Method. *International Journal of Molecular Science*, **13**, 6639-6650. https://doi.org/10.3390/ijms13066639

[37] Lakshmanan, B. (1968) Infrared Absorption Spectrum of Sodium Citrate. *Journal of the Indian Institute of Science*, **39**, 108-120.

[38] Ghosh, M.K., Wahed, M.I.I., Ali, M.A. and Barman, R.K. (2019) Formulation and Characterization of Fenofibrate Loaded Solid Dispersion with Enhanced Dissolution Profile. *Pharmacology & Pharmacy*, **10**, 343-355. https://doi.org/10.4236/pp.2019.107028

[39] Karavas, E., Georgarakis, E., Sigalas, M.P., Avgoustakis, K. and Bikiaris, D. (2007) Investigation of the Release Mechanism of a Sparingly Water-Soluble Drug from Solid Dispersions in Hydrophilic Carriers Based on Physical State of Drug, Particle Size Distribution and Drug-Polymer Interactions. *European Journal of Pharmaceutics and Biopharmaceutics*, **66**, 334-347. https://doi.org/10.1016/j.ejpb.2006.11.020

[40] Maheshwari, R.K. and Jagwani, Y. (2011) Mixed Hydrotropy: Novel Science of Solubility Enhancement. *Indian Journal of Pharmaceutical Science*, **73**, 179-183. https://doi.org/10.4103/0250-474X.91585

[41] Das, S., Roy, P., Auddy, R.G. and Mukherjee, A. (2011) Silymarin Nanoparticle Prevents Paracetamol-Induced Hepatotoxicity. *International Journal of Nanomedicine*, **6,** 1291-1301. https://doi.org/10.2147/IJN.S15160

[42] Kelava, T., Ćavar, I. and Čulo, F. (2010) Influence of Small Doses of Various Drug Vehicles on Acetaminophen-Induced Liver Injury. *Canadian Journal of Physiology and Pharmacology*, **88**, 960-967. https://doi.org/10.1139/Y10-065

[43] Ghosh, M.K., Wahed, M.I.I., Khan, R.I., Habib, A. and Barman, R.K. (2020) Pharmacological Screening of Fenofibrate Loaded Solid Dispersion in Fructose Induced Diabetic Rat. *Journal of Pharmacy and Pharmacology*, **72**, 909-915. https://doi.org/10.1111/jphp.13267

[44] Kushida, I., Ichikawa, M. and Asakawa, N. (2002) Improvement of Dissolution and Oral Absorption of ER-34122, a Poorly Water-Soluble Dual 5-Lipoxygenase/Cyclo-

oxygenase Inhibitor with Anti-Inflammatory Activity by Preparing Solid Dispersion. *Journal of Pharmaceutical Sciences*, **91**, 258-266. https://doi.org/10.1002/jps.10020

[45] Law, S.L., Lo, W.Y., Lin, F.M. and Chaing, C.H. (1992) Dissolution and Absorption of Nifedipine in Polyethylene Glycol Solid Dispersion Containing Phosphatidylcholine. *International Journal of Pharmaceutics*, **84**, 161-166. https://doi.org/10.1016/0378-5173(92)90056-8

[46] Laitinen, R., Löbmann, K., Strachan, C.J., Grohganz, H. and Rades, T. (2013) Emerging Trends in the Stabilization of Amorphous Drugs. *International Journal of Pharmaceuti*, **453**, 65-79. https://doi.org/10.1016/j.ijpharm.2012.04.066

[47] Bhattacharya, S. and Suryanarayanan, R. (2009) Local Mobility in Amorphous Pharmaceuticals-Characterization and Implications on Stability. *Journal of Pharmaceutical Sciences*, **98,** 2935-2953. https://doi.org/10.1002/jps.21728

[48] Lehmkemper, K., Kyerematen, S.O., Heinzerling, O., Degenhardt, M. and Sadowski, G. (2017) Long-Term Physical Stability of PVP- and PVPVA-Amorphous Solid Dispersions. *Molecular Pharmaceutics*, **14**, 157-171. https://doi.org/10.1021/acs.molpharmaceut.6b00763